Theoretical investigation on the interactions between HRnCCH and X(X=N$_2$, O$_2$, H$_2$O, NH$_3$)

Yu-Hua Han[a], Zheng-Wen Long[a,*], Bo Long[a,b,*], Chao-Yun Long[a], Shao-Hong Cai[a], and Wei-Jun Zhang[c]

[a] *Department of Physics, Guizhou University, Guiyang 550025, China*
[b] *College of Computer and Information Engineering, Guizhou University for Nationalities, Guiyang 550025, China*
[c] *Laboratory of Environment Spectroscopy, Anhui Institute of Optics and Fine Mechanics, Chinese Academy of Sciences, Hefei 230031, China*

Abstract. We have investigated the structures and properties of the hydrogen bonded complexes formed between HRnCCH and X (X stand for nitrogen, oxygen, water and ammonia) using MP2 (full) theoretical method at the aug-cc-pVTZ-pp for Rn atom and aug-cc-pVTZ for other atoms. In this study, as for the complexes between HRnCCH and X, three stationary structures are located (one annular and two linear structures) corresponding to the true energy minima on the potential energy surface. In these complexes, the red shift of the H-Rn stretch in the linear structure C$_{XA}$, whereas the blue shift of the H-Rn stretch in the structure linear C$_{XB}$ and the structure circular C$_{XC}$, the biggest red shift is -35.71 cm^{-1} in C$_{NH3A}$ and the biggest blue shift is 76.45 cm^{-1} in C$_{H2OB}$. In addition, we found a tremendous red shift in C$_{H2OC}$ (-154.7 cm^{-1} in O–H bond) and C$_{NH3A}$ (-96.15 cm^{-1} in C–H bond). The most stable structure is the circular structure between HRnCCH and H$_2$O, whose interaction energies is -27.4 kJ/mol. The origin of the frequency shift and charge transfer in these complexes has been analyzed by the natural bond orbital analysis and atom in molecule. The natural bond orbital analysis indicates the C$\rightarrow\sigma^*_{H-Rn}$ orbital interaction plays a key role in the stabilization energy. The atom in molecule shows the largest the absolute value of $V = 0.0220$ a.u and the most negative the value of $H = -0.0055$ a.u corresponding the most stabilization of the circular structure between HRnCCH and H$_2$O.

Corresponding author. Email addresses: `sci.zwlong@gzu.edu.cn` (Z. W. Long); `wwwltcommon@sina.com` (B. Long)

1 Introduction

Hydrogen bonding is one of the weak forces between van der Waals force and covalent bond, which plays an important role in chemistry, biology and physics [1–3]. The type of the hydrogen bond is X-H⋯Y, where X and Y are electronegative atoms (such as F, O, and N [4–6]) or groups. For the past decades, the hydrogen bonding has been extensively studied by experimental [7] and computational methods. The first studies focused on the hydrogen bond (H–X) for the characteristics of the red-shift of stretch vibration. For example, ab initio methods have been employed to investigate the relations among bond distances, interaction energies and frequency shifts [8]. Later, researchers began to study their characteristics of structure, the charge transfer and interaction energy [9]. In particular, the blue shift hydrogen bonds have obtained an increasing interest for recent years [10–13]. In addition, hydrogen bonding has been applied to the macromolecular, such as the hydrogen bonding changes in stresses environmental [14] and the application in molecular recognition [15–17]. Additionally, one has explored the natures and features of hydrogen bond and halogen bond [18, 19].

On the other hand, although it is well known that the single noble-gas cannot participate in chemical reaction, it can be inserted into other molecules, leading to formation of the metastable complex by photolyzing HY molecules at the low temperature rare gas and thermally mobilizing H atoms [20]. In 1962, the first noble-gas compound has been discovered by Barlett [21]. Some natures and features of neutral noble-gas molecules HNgY (Ng = noble gas atom, Y = electronegative atom or group) have been explored. The HNgY molecule has an ionic bond (Ng–Y) and a covalent bond (H–Ng), and has a very large dipole moment. Thus, these molecules are very easy to form hydrogen bonded complexes [22]. After the first stable neutral noble-gas compound HArF [23, 24] studied, the complexes between HKrF [25], HKrCl [26] and N_2 [27], P_2 and CO had been studied by theoretical and experimental methods. Large red-shift in the HArF⋯P_2 [28] complex was unveiled. Recently, the features and natures of FArCCH [29, 30], HArCCH and HArCCF [31] have been explored by theoretical methods. The gigantic blue-shift (574 cm^{-1}) of the H-Ar stretching frequency in C_2H_2⋯HArCCF complex [32] was observed. Hanna Tanskanen have studied the HXeCCH⋯CO_2 complex [33] using theoretical calculations, which have found blue-shift and red-shift, respectively. According to the latest reports, HRnCCH [34] was probably existed in the atmosphere by theoretical investigation.

In this study, the complexes formed between HRnCCH and X (X=N_2, O_2, H_2O, NH_3) using the MP2 theoretical method at the aug-cc-pVTZ-pp level for the first time. In addition, the natures and characters of the bond critical points have been analyzed using the natural bond theory and quantum theory of atom in molecules. The purpose of this study is to elucidate the structures of these complexes and obtain the stabilization energies of the complexes reported here. Furthermore, this study provides a new insight on the Rn atom to affect the natures of the molecule.

2   Computational methods

The electronic structure calculations are carried out using the Gaussian09 package of computational codes [35]. Harmonic geometry optimization and vibrational frequencies of complexes and isolated monomers are optimized using the second order Møller-Plesset perturbation theory (MP2). The augmented Dunning's correlation consistent valence triple -zeta aug-cc-pVTZ basis sets are applied for all atoms except Rn. For Rn atoms, the pertinent potential effect is used. The computational method in this study was previously applied for other complexes about Rn atom [34]. The minimum energy nature of the optimized structures is verified using the vibrational frequency analysis. The interaction energies are obtained at the same level of theory and calculated by subtracting the energies of the complex to the energies of the isolated compounds. The nature bond orbital (NBO) analyses are carried out using the NBO package included in the Gaussian 09 suite of programs [36]. AIM calculations are carried out using the wave functions, generated from the MP2/aug-cc-pVTZ-pp calculations with the AIM2000 [37].

3   Results and discussion

3.1   Geometrical parameters, interaction energies and vbration frequencies

Fig. 1 shows the structures of the complexes between HRnCCH and X. There have been three distinct structures between HRnCCH and X, which involve two approximately linear structures and one circular structure. The structure HRnCCH$\cdots$X and the X$\cdots$HRnCCH are denoted C_{XA}, C_{XB} respectively, while the ring structure is expressed as C_{XC}. It is noted that the complex (C_{N2B}) N2$\cdots$HRnCCH is not a linear structure with the bond angle ($\angle$HNN) of 151.0°, whereas in the complex (C_{O2A}) the molecular oxygen is about perpendicular to the HRnCCH.

Table 1 presents the interaction energies of the complexes between HRnCCH and X. The linear configurations (C_{XA} and C_{XB}) in the complexes are less weakly bound than the circular structure (C_{XC}). The interaction energies of C_{XA} complexes are stronger than those of the C_{XB}, except HRnCCH$\cdots$NH$_3$ complex. The energy of C_{H2OA} is -6.4 kJ/mol and C_{H2OB} is -3.8 kJ/mol [38], but the complex of HCCH$\cdots$H$_2$O (linear) is -3.3 kJ/mol at 6-31G** level and -4.5 kJ/mol at MP2/6-31G** level. The energy of C_{NH3A} is -8.02 kJ/mol and C_{NH3B} is -10.64 kJ/mol, whereas HCCH$\cdots$NH$_3$ complex is -4.0 kJ/mol at 6-31G** level and -5.3 kJ/mol

Table 1: Electronic interaction energies of the complexes HRnCCH between X (X=N$_2$, O$_2$, H$_2$O and NH$_3$) (in kJ/mol)*.

	C_{XA}	C_{XB}	C_{XC}
E_{N2}	-3.27	-2.86	-10.00
E_{O2}	-4.61	-2.99	-5.71
E_{H2O}	-6.43	-3.81	-27.43
E_{NH3}	-8.02	-10.64	-23.77
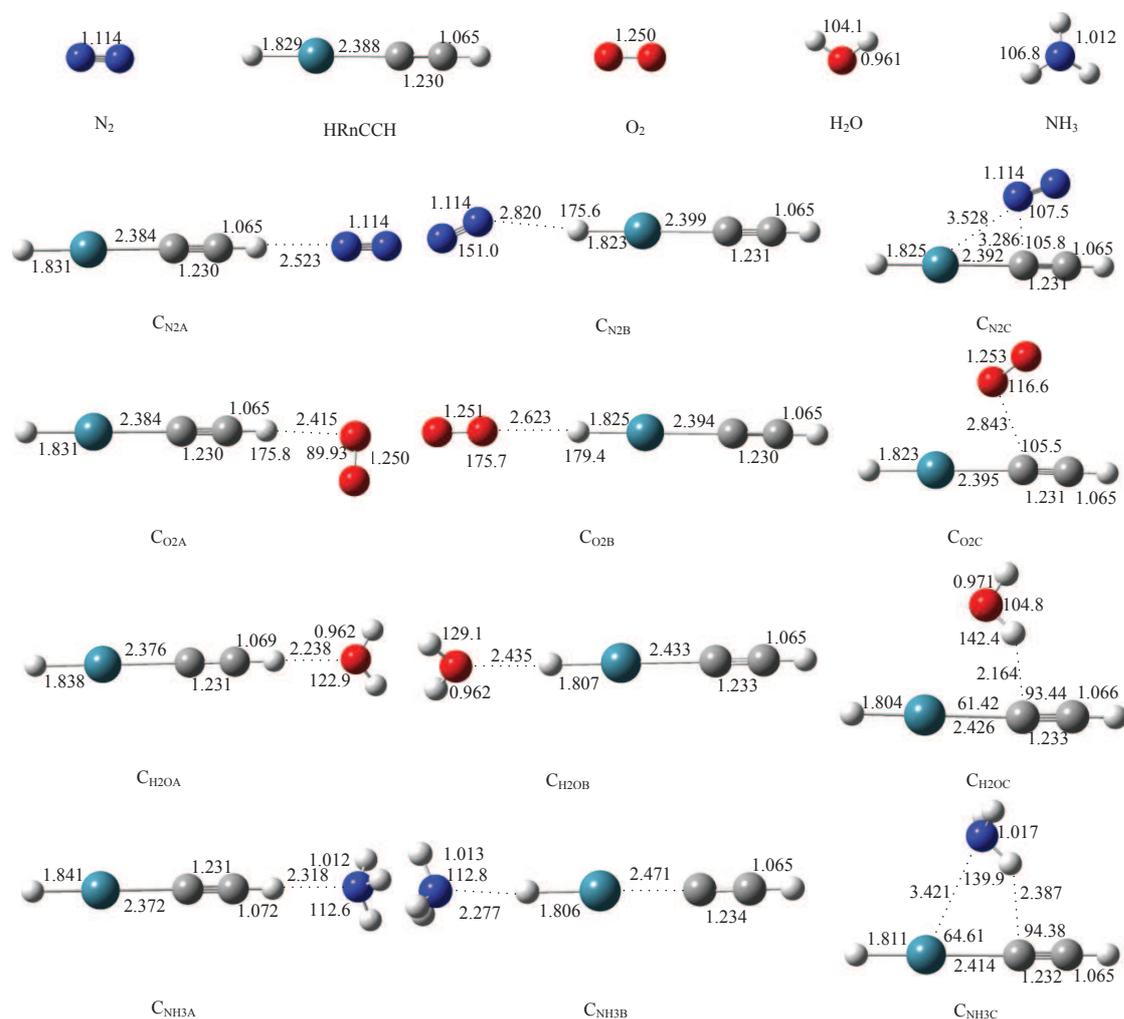
Figure 1: Computational structures of the complexes between HRnCCH and X (X=N$_2$, O$_2$, H$_2$O and NH$_3$). The values of bond lengths and angle are in Å and degrees, respectively.

at MP2/6-31G** [38] level. The result shows that the interaction energy changes stronger because of the insertion of Rn atom into the H–C bond.

The interaction distances in structures C$_{XA}$ range from 2.238 Å to 2.523 Å; 2.277 Å to 2.820 Å in C$_{XB}$, and 2.164 to 3.286 Å in C$_{XC}$, respectively. From geometrical point of view, the optimized geometries show that the Rn atom exerts a minor influence on C$_{XA}$, compared with complexes HCCH⋯Y(Y=H$_2$O, NH$_3$), where the hydrogen bond distances are in the range 2.197 Å–2.218 Å [38]. However, it is worth noting that the binding distance in the linear complexes HRnCCH and N$_2$ is calculated to be 2.519 Å, which is shorter than that in the

HCCH···N_2 (4.753 Å [39]). Table 2 displays the variations of binding distance between complex and monomers. It is indicated that the variation of $R_{(H-Rn)}$ and $R_{(Rn-C)}$ is obviously in the range -0.025 Å–0.012 Å and -0.016 Å – 0.083 Å. The change of $\Delta R_{(C-C)}$ bond and $\Delta R_{(C-H)}$ bond is very subtly because the largest value is 0.003 Å and 0.007 Å, respectively. In ring HRnCCH···O_2 complex, the H–Rn bond is shortened a little, whereas the Rn–C bond is elongated. The change of the H–Rn bond length is smaller than Rn–C bond length, the same situation can also be founded in other complexes.

Table 3 displays the change of the vibration frequency. All the N-N/H bonds and O–O/H bonds stretch vibration shift to low frequency (red shift). The change value in the circular structure is more larger than others especially in the C_{H2OC} complex, which is (-154.7 cm^{-1}) about twelve times as much as that in the C_{H2OB} compound. The large red-shift corresponds

Table 2: The bonds length variations between complexes and monomers (Å).

	$\Delta R_{(N-N)}$	$\Delta R_{(O-O)}$	$\Delta R_{(H-Rn)}$	$\Delta R_{(Rn-C)}$	$\Delta R_{(C-C)}$	$\Delta R_{(C-H)}$	$R_{(H/C-N/O)}$
C_{N2A}	0.000	0.000	0.002	-0.004	0.000	0.000	2.523
C_{N2B}	0.000	0.000	-0.006	0.011	0.001	0.000	2.820
C_{N2C}	0.000	0.000	-0.004	0.004	0.001	0.000	3.286
C_{O2A}	0.000	0.000	0.002	-0.004	0.000	0.000	2.415
C_{O2B}	0.000	0.001	-0.004	0.006	0.000	0.000	2.623
C_{O2C}	0.000	0.003	-0.006	0.007	0.000	0.000	2.843
C_{H2OA}	0.000	0.001	0.009	-0.012	0.001	0.004	2.238
C_{H2OB}	0.000	0.001	-0.022	0.045	0.003	0.000	2.435
C_{H2OC}	0.000	0.01	-0.025	0.038	0.003	0.001	2.164
C_{NH3A}	0.000	0.000	0.012	-0.016	0.001	0.007	2.318
C_{NH3B}	0.001	0.000	-0.023	0.083	0.004	0.000	2.277
C_{NH3C}	0.005	0.000	-0.018	0.026	0.002	0.000	2.387

Table 3: The vibrational frequencies (cm^{-1}) change between complexes and monomers.

	$\Delta v_{(N-N/H)}$	$\Delta v_{(O-O/H)}$	$\Delta v_{(H-Rn)}$	$\Delta v_{(Rn-C)}$	$\Delta v_{(C-C)}$	$\Delta v_{(C-H)}$
C_{N2A}	-0.52		-6.92	5.98	0.34	7.89
C_{N2B}	-3.56		27.92	-2.71	-2.56	-0.02
C_{N2C}	-4.94		8.28	-2.25	-3.55	-2.32
C_{O2A}		-4.34	-7.06	7.10	0.08	2.66
C_{O2B}		-11.08	27.72	-1.64	-1.45	0.23
C_{O2C}		-27.75	15.65	-2.68	-7.27	-3.96
C_{H2OA}		-8.41	-28.20	15.05	-2.04	-42.35
C_{H2OB}		-13.69	76.45	-12.22	-12.29	-2.57
C_{H2OC}		-154.70	69.84	-16.56	-13.38	-9.88
C_{NH3A}	-4.08		-35.71	16.62	-8.62	-96.15
C_{NH3B}	-10.24		11.60	-21.33	-22.65	-5.46
C_{NH3C}	-41.55		46.51	-13.93	-10.99	-7.72

to one of the biggest bond length change of -0.01 Å. In H–Rn bond, the unique red-shift in C_{XA} complex is found, which is calculated to be -6.92cm^{-1} in the structure HRnCCH$\cdots$N$_2$ complex, -7.06cm^{-1} in the structure C_{O2A}, -28.2 cm^{-1} in the structure C_{H2OA}, -35.71 cm^{-1} in the structure C_{NH3A}, whereas the unique blue-shift appears in structure C_{XB} and C_{XC}. The biggest is 76.45 cm^{-1} in C_{H2OB} complex. In addition, in the HRnCCH$\cdots$H$_2$O and HRnCCH$\cdots$NH$_3$ complex the H–Rn bond is shortened, whereas the Rn–C bond is elongated. The C–C and C–H bonds are always red-shift in HRnCCH$\cdots$H$_2$O and HRnCCH$\cdots$NH$_3$ complexes. The huge red-shift in C-H bond is calculated to be -42.35cm^{-1} in the HRnCCH$\cdots$H$_2$O complex, whereas it is -96.15cm^{-1} in the HRnCCH$\cdots$NH$_3$ complexe, which is accompanied the bond length change by 0.004 Å and 0.007 Å, respectively.

3.2 Natural bonding orbital (NBO) analyses

In order to better understanding the frequency shifts and nature of the interaction in these complexes, the natural bonding orbital (NBO) analyses have been carried out to study the complexes, at the MP2/ aug-cc-pVTZ-pp level. The results are summarized in Table 4. In all the orbital interaction between the acceptor orbital and the donor orbital, the C$\rightarrow \sigma^*_{H-Rn}$ orbital interaction plays a key role in the stabilization energy. The change of stabilization energy in complexes HRnCCH and X (X=O$_2$, N$_2$) is very small, whereas the value ranges from 24.04 kJ/mol to 33.25 kJ/mol in the complexes between HRnCCH and H$_2$O and from 20.00 kJ/mol to 33.84 kJ/mol in the complex between HRnCCH and NH$_3$, respectively. In the structure C_{XA}, the stabilization energy is the largest, while the value in the structure C_{XB} is the smallest. The stabilization energy displays the ability of transfer electron: the bigger of the stabilization energy, the more charges transfer from C atom to H–Rn bond. Therefore, the most charge transfers from C atom to σ^*_{H-Rn} orbital in C_{NH3C} complex from Table 4. There are a little different about the stabilization energy and the charge transfer direction in HCCH$\cdots$NH$_3$ compound, which corresponds -54.52 kJ/mol and O$\rightarrow$N–H orbital interaction [40].

The charge on the H atom is negative, which becomes more negative in C_{XA}, whereas the charge on the C atom is negative, which becomes fewer in all the compounds except C_{O2C} complex. In the complexes, the electron density in H–Rn bond in increased, ranging from 0.00342 to 0.02073 e in the structure C_{XA}, whereas the electron density is decreased in H–Rn bond, which ranged from -0.06032 to -0.00623 e and from -0.04435 to -0.00268 e in the structure C_{XB} and structure C_{XC}, respectively. Furthermore, the loss of the electron density in absolute value at the structure C_{XB} is larger than that of the structure C_{XA} and the structure C_{XC}. It is proved that the decrease of electron density in the σ^*_{H-Ar} orbital corresponds to blue-shift hydrogen bonded N$_2\cdots$HArF complex, whereas an increase in the σ^*_{H-Ar} orbital electron density of red-shift hydrogen bonded P$_2\cdots$HArF complex [41]. Thus, we could understand that the negative value of the $\Delta\sigma^*_{H-Rn}$ is responsible for the blue shift of the H-Rn stretch in the structure C_{XA}, whereas the positive value of $\Delta\sigma^*_{H-Rn}$ is reflected the red shift of the H-Rn stretch in the structure C_{XB} and the structure C_{XC}.

Table 4: Stabilization energy (E_{ij}, kJ/mol), changes in selected atom charges (Δq, e) and selected orbital occupancies in the complexes at the MP2/ aug-cc- pVTZ-pp level*.

	E_{ij} (kJ/mol)	Δq_H	Δq_C	$\Delta\sigma^*_{H-Rn}$
C_{N2A}	31.47	-0.00407	-0.00270	0.00343
C_{N2B}	29.05	0.01595	-0.00375	-0.01001
C_{N2C}	30.18	0.00448	-0.00039	-0.00492
C_{O2A}	31.33	-0.00412	-0.00090	0.00342
C_{O2B}	29.71	0.00839	-0.00274	-0.00623
C_{O2C}	30.24	0.00353	0.00888	-0.00268
C_{H2OA}	33.25	-0.01955	-0.02463	0.01688
C_{H2OB}	24.04	0.08502	-0.01592	-0.04690
C_{H2OC}	25.16	0.04229	-0.01850	-0.04435
C_{NH3A}	33.84	-0.02397	-0.02951	0.02073
C_{NH3B}	20.00	0.13228	-0.02551	-0.06032
C_{NH3C}	26.82	0.02646	-0.00257	-0.03074

* E_{ij} is the stabilization energy due to the C→σ^*_{H-Rn} orbital interaction. Δq is representing the different charge of complex and monomer. $\Delta\sigma^*_{H-Rn}$ is the different charge of complex and monomer at H–Rn bond.

Table 5: Topological properties of the bond critical points of the HRnCCH···N_2, HRnCCH···O_2, HRnCCH···H_2O and HRnCCH···NH_3 complexes at the MP2/aug-cc-pVTZ level of theory*.

Compound	Bond/ring	r^a	ρ(au)^b	$\nabla^2\rho$(au)^c	G(au)^d	V(au)^e	H(au)^f
C_{N2A}	H2N6	2.523	0.0072	-0.0286	0.0055	-0.0039	0.0016
C_{N2B}	H5N7	2.820	0.0053	-0.0163	0.0032	-0.0024	0.0008
C_{N2C}	Rn4N7	3.528	0.0068	-0.0243	0.0048	-0.0035	0.0013
	C3N7	3.286	0.0056	-0.0199	0.0039	-0.0027	0.0012
C_{O2A}	H2O1	2.415	0.0184	-0.0225	0.0064	-0.0072	-0.0008
C_{O2B}	H5N7	2.623	0.0104	-0.0268	0.0059	-0.0051	0.0008
C_{O2C}	C3O1	2.843	0.0295	-0.0391	0.0120	-0.0142	-0.0022
C_{H2OA}	H2O1	2.238	0.0265	-0.0450	0.0125	-0.0137	-0.0012
C_{H2OB}	H5O1	2.435	0.0183	-0.0339	0.0085	-0.0086	-0.0001
C_{H2OC}	C3H5	2.164	0.0339	-0.0441	0.0165	-0.0220	-0.0055
C_{NH3A}	H2N7	2.318	0.0143	-0.0448	0.0098	-0.0085	0.0013
C_{NH3B}	H5N6	2.277	0.0187	-0.0479	0.0110	-0.0101	0.0009
C_{NH3C}	Rn4N7	3.421	0.0101	-0.0312	0.0066	-0.0054	0.0012
	C3H5	2.387	0.0129	-0.0386	0.0087	-0.0078	0.0009

* a: the distance of hydrogen bonding; b: Electronic charge density at the critical point; c: Laplacian of the electron density at the bond critical point; d: Kinetic electron density at the bond critical point; e: Potential electron energy density at the bond critical point; f: Total electron energy density at the bond critical point.

3.3 Topological analysis

Table 5 lists the binding distance intermolecular, the electron density, the Laplacian of the electron density, the densities of kinetic energy, potential energy and total energy ($H=G+V$) at

bond critical points located between two monomers. In all the systems studied here, the value of electron density is relatively small, and the Laplacian of the electron density is negative. According to Bader and Essën [42], the negative value of the Laplacian of the electron density, occurs in shared interactions, displays the electron density concentrated and the potential energy dominates both the local total electronic energy and the local virial relationship.

In Table 5, it can be seen that the absolute value of the potential energy density is larger than the kinetic energy density, which leads to values of total energy is negative. Exceptions are hydrogen complexes formed with nitrogen and ammonia complexes, in which the kinetic energy density is larger than the potential energy density, total energy is positive. According to the theory of Cremer and Kraka [43], indicates the larger the absolute value of the potential energy density and the more negative the value of total electronic energy, the more stabilization of the structure. Thus, the most stable complex is C_{H2OC} (the value of total electronic energy is -0.0055 a.u), whereas the most unstable complex is C_{N2A} (the value of total electronic energy is 0.0016 a.u).

4   Conclusions

In this work, we have studied the complexes between HRnCCH and X (X $=$ N$_2$, O$_2$, H$_2$O, NH$_3$) by ab initio methods at MP2/ aug-cc-pVTZ level. Three structures are found for the interaction between HRnCCH and X: one circular and two linear structures. The computed H-Rn bond stretching frequencies are red-shifted by -6.92 cm^{-1}, -7.06 cm^{-1}, -28.20 cm^{-1}, -35.71 cm^{-1} for the linear structure C_{XA}, respectively. For structure C_{XB} and structure C_{XC}, the H–Rn bond stretching values are blue shifted and the biggest is 76.45 cm^{-1} in C_{H2OB}. Furthermore, a very large red shift is reported in C_{H2OC} (-154.7 cm^{-1} in O–H bond) and C_{NH3A} (-96.15 cm^{-1} in C–H bond).

The circular structure C_{XC} has the largest interaction energy (-27.43 kJ/mol for C_{H2OC} complex, specifically), whereas the other two linear structures are weakly bonded. Thus, the structure C_{XC} is the most stable configuration. In these complexes, the electron density in the $\Delta\sigma^*_{H-Rn}$ orbital of structure C_{XC} is increased, whereas the other two linear structures are decreased. In all the orbital interaction between the acceptor orbital and the donor orbital, the C$\rightarrow\sigma^*_{H-Rn}$ orbital interaction plays a key role in the stabilization energy. The Laplacian of the electron densities in all the complexes are negative value, which occurs in shared interactions, displaying the electron density concentrated.

References

[1] G. Gilli and P. Gilli, The Nature of the Hydrogen Bond (Oxford University Press, Great Clarendon Street, 2009).

[2] A. Novak, Struct. Bonding 18 (1974) 177.

[3] S. J. Grabowski, Hydrogen Bonding-New Insights: Challenges and Advances in Computational Chemistry and Physics (Springer Netherlands, Amsterdam, 2006).

[4] G. A. Jeffrey and W. Saenger, Hydrogen Bonding in Biological Structures (Springer, Berlin, 1991).

[5] S. Scheiner, Molecular Interactions: From van der Waals to Strongly Bound Complexes (Wiley, Chichester, 1997).

[6] G. R. Desiraju and T. Steiner, The Weak Hydrogen Bond in Structural Chemistry and Biology (Oxford University Press, Oxford, 1999).

[7] C. E. H. Dessent and K. M. Dethlefs, Chem. Rev. 100 (2000) 3999.

[8] A. Y. Li, J. Phys. Chem. A 110 (2006) 10805.

[9] P. Hobza and Z. Havlas, Chem. Rev. 100 (2000) 4253.

[10] A. Karpfen and E. S. Kryachko, J. Phys. Chem. A 107 (2003) 9724.

[11] J. Joseph and E. D. Jemmis, J. Am. Chem. Soc. 129 (2007) 4620.

[12] S. Scheiner and T. Kar, J. Phys. Chem. A 106 (2002) 1784.

[13] E. Mrazkova and P. Hobza, J. Phys. Chem. A 107 (2003) 1032.

[14] M. J. Ski and M. Sol, J. Phys. Chem. A 114 (2010) 10253.

[15] S. Chang, J He, A. Kibel, *et al.*, Nature Nanotechnol. 4 (2009) 297.

[16] T. Reid, Nature Chem. 1038 (2009) 204.

[17] S. C. Li, L. N. Chu, X. Q. Gong, and U. Diebold, Science 328 (2010) 882.

[18] W. Wang, Y. Zhang, and B. Ji, J. Phys. Chem. A 114 (2010) 7257.

[19] N. J. M. Amezaga, S. C. Pamies, N. M. Peruchena, and G. L. Sosa, J. Phys. Chem. A 114 (2010) 552.

[20] L. Khriachtchev, M. Räsänen, and R. B. Gerber, Acc. Chem. Res. 42 (2009) 183.

[21] N. Bartlett, Proc. Chem. Soc. 6 (1962) 218.

[22] S. Y. Yen, C. H. Mou, and W. P. Hu, Chem. Phys. Lett. 383 (2003) 606.

[23] L. Khriachtchev, M. Pettersson, N. Runeberg, *et al.*, Nature 406 (2000) 874.

[24] L. Khriachtchev, M. Pettersson, A. Lignell, and M. Räsänen, J. Am. Chem. Soc. 123 (2001) 8610.

[25] M. Pettersson, L. Khriachtchev, A. Lignell, and M. Räsänen, J. Chem. Phys. 116 (2002) 2508.

[26] S. A. C. McDowell, J. Chem. Phys. 119 (2003) 3711.

[27] A. Lignell, L. Khriachtchev, M. Pettersson, and M. Räsänen, J. Chem. Phys. 118 (2003) 11120.

[28] S. A. C. McDowell, Phys. Chem. Chem. Phys. 5 (2003) 808.

[29] M. Solimannejad and S. Scheiner, J. Phys. Chem. A 109 (2005) 6137.

[30] S. A. C. McDowell, Mol. Phys. 102 (2004) 1441.

[31] S. Li, A. Cohen, and R. B. Gerber, J. Am. Chem. Soc. 128 (2006) 7156.

[32] J. B. Cheng, Y. L. Wang, Q. Z. Li, Z. B. Liu, W. Z. Li, and B. A. Gong, J. Phys. Chem. A 113 (2009) 5235.

[33] H. Tanskanen, S. Johansson, A. Lignell, *et al.*, J. Chem. Phys. 127 (2007) 154313.

[34] E. Tsivion and R. B. Gerber, Phys. Chem. Chem. Phys. 12 (2010) 11791.

[35] M. J. Frisch, G. W. Trucks, H. B. Schlegel, *et al.*, Gaussian 09, Rev. A.02 (Gaussian Inc., Wallingford, CT, 2009).

[36] E. D. Glendening, A. E. Reed, J. E. Carpenter, and F. Weinhold, NBO Version 3.1 (Gaussian, Inc., Pittsburgh, PA, 1992).

[37] F. Biegler-König and J. Schönbohm, AIM 2000, Version 2 (Bieledeld, Germany, 2002).

[38] X. J. Yan, S. M. Wang, M. Hodošček, and G. W. A. Milne, J. Mol. Struct. 309 (1994) 279.

[39] K. A. Franken and C. E. Dykstra, J. Phys. Chem. 97 (1993) 11408.

[40] S. A. C. McDowell, Phys. Chem. Chem. Phys. 5 (2003) 808.

[41] Y. Yang, W. J. Zhang, S. X. Pei, *et al.*, J. Mol. Struct. (Theochem.) 725 (2005) 133.

[42] R. F. W. Bader, and H. Essén, J. Chem. Phys. 80 (1984) 1943.

[43] D. Cremer and E. Kraka, Angew. Chem. Int. Ed. 23 (1984) 627.